Forced 2-D Energy Transitions Suitable for High Power Applications

Gary L. Viviani, *Senior Member, IEEE*

***Abstract*— Transitioning from one energy state to another, in a highly controlled manner, is a vexing problem for high power applications. In high power microwave, lasers, plasmas, and related situations there is often a need to create high power pulse trains with well-defined and as narrow as possible pulsewidths. Single one-shot pulses are also of interest. The resulting formulation allows for flexible and controllable pulse shape, duration, and periodicity. It provides for an optimal means for rapid transitions from low energy states to high energy ones. The essence of the approach stems from being able to describe pulse formation as 2-D switching in the phase plane for the associated dynamics of interest. Such a formulation is applicable to a wide array of situations beyond the electronic ones that are actually synthesized in order to confirm the underlying theory. A mathematical proof is also provided.**

***Index Terms*— Multi-stable oscillator, nonlinear dynamical systems, pulse shaping methods, pulsed power, quantization.**

I. Introduction

THE complications of transferring large amounts of charge, quickly, are most apparent when considering high power applications such as high power microwave (HPM) [1], high power lasers, plasma discharges, or else rail gun devices. Other examples are possible [2]. When this situation exists, it often leads to a related concept which is referred to as pulse shaping or else pulse compression. The principal concern is often to make a "pulse" of charge that is as narrow as possible with a magnitude that is as large as possible in order to deliver maximum power with minimal energy. Mastering the necessary switching speeds has significant practical application.

In order to form a pulse, there must be two changes in charge (flux) momentum. This requires forces in at least two opposing directions. It makes sense to characterize the required force as a vector in the plane. In the case of electrodynamic phenomena, the units are typically voltage and current. The I–V relationship is identical in scale to a dynamical phase plane representation. This means the dynamics can be superimposed on the I–V characteristic.

For electrodynamic phenomena, it is necessary to draw upon nonlinear dynamics in order to characterize the flow of charge in the plane. The mathematics of nonlinear dynamical equations, in the spirit of Poincaré [3], are renowned and well established. The dynamical flows in the plane have been comprehensively investigated in the spirit of extending the work of Poincaré in an industrial manner [4]–[7]. Such a plane is equivalent to a complex one.

A periodical flow in a plane can also be thought of as an oscillation, assuming it is stable. This is true for all forms of matter. The underpinnings of solutions to the wave equation can be considered as (stable) periodical flows. It is well known that under a variety of conditions, solutions to the Schrödinger Equation are, indeed, periodic [8]. Taking advantage of this knowledge will be a primary consideration in what follows.

In a mathematical system as well as in eletrodynamic one, such as a plasma, an *oscillation* necessitates a nonlinearity. For electronic systems, the nonlinearity takes the form of "negative resistance." For systems that arise in a multiplicity or substances, the generalization of the concept of negative resistance can be determined from [9]. A principal result of this work will be to demonstrate that a nonlinearity-dependent oscillator is an essential building block to achieve optimal performance associated with pulse formation.

At high energy levels, there is often an interest in discharges as (for example) described in [10]. While discharge is often the terminology that is applied, there are many cases where pulse trains (sequential discharges) are actually desired. In this case, the concept of an oscillator comes to mind. Ideally, a high energy oscillator (pulse train) would be developed. Some investigations into plasma oscillations have occurred, such as [11]. A periodic sequence corresponding to a stable solution for an electrodynamic charge flow (or discharge) must result from an initial condition consistent with a stable flow. Such a situation is necessary (but not sufficient) for a stable *oscillation* to exist. Moreover, if an electrodynamic flow is going to change from one (average) energy level to another, then the end state must also be an oscillation, assuming stability is desired. An "explosive" end state such as a conventional discharge can exist [10], but this would imply a "one-shot" operation. For the purpose of this paper, and to be consistent with the concept of pulse shaping, only stable flows in the plane are considered. These must, therefore, be periodic.

If one imagines that a stable oscillation exists, it is possible to think in terms of higher power outputs by constraining the pulsewidth to be as small as possible and the amplitude as high as possible. This will be the focus of this paper. Alternatively, and possibly in conjunction with pulse shaping, it is possible to apply the concept of stochastic resonance [12] to plasmas

Manuscript received November 21, 2018; revised April 9, 2019; accepted May 22, 2019. Date of current version July 9, 2019. The review of this paper was arranged by Senior Editor R. P. Joshi.

The author is with the FAST Labs, BAE Systems, Austin, TX 78725 USA (e-mail: gary.viviani@baesystems.com).

Color versions of one or more of the figures in this paper are available online at http://ieeexplore.ieee.org.

Digital Object Identifier 10.1109/TPS.2019.2920588

as well as electronic oscillators. Stochastic resonances in plasmas are evaluated in [13]. In order to understand stochastic resonance, it is necessary to understand the underlying periodical phenomena that are the focus of this paper. Stochastic resonance remains a possible means to further amplify what is described, but it is dependent upon stationary dynamics.

What is presented in the rest of this paper will be a formal mathematical characterization of how to go about creating pulse trains of potentially high power from the perspective of a multi-state oscillator. In principle, the mathematics and associated electrodynamics can be applied in a variety of circumstances involving various substances as described in [9]. The concept of "negative resistance" oscillations includes those attributable to plasmas, as such a nonlinearity is a prerequisite to any oscillation. For convenience, a lower power electronic development is pursued. The principles are easier to confirm with more convenient components. Extensions to high power electronic pulses (and pulse trains) used to drive lasers, microwave, and devices such as rail guns are inferred as the formulation is completely general. Other electrodynamic applications, such as plasmas, are best viewed through the lens of an equivalent circuit, like what is demonstrated in [14].

If we wish to address the fastest *stable* switching times, then we must address the situation of transitioning from one stable oscillation to another, regardless of the substances under consideration. Here, the term stable oscillation is employed in contrast to the alternative "stable fixed point" in the phase plane. The point is that working with stable oscillations, versus the more typical stable fixed points, is the basis for superior performance. The reasoning behind this will become apparent.

A primary reason that this approach is not typically pursued is because the means for transitioning from one stable oscillation to another are not generally understood (with only a change in initial conditions). In turn, this capability is predicated on the existence of multiple stable periodical equilibriums. As will be described, the condition of multiple stable periodical equilibriums is directly associated with a certain type of phase plane nonlinearity. An electronic synthesis is provided and shown to confirm the theory which is mathematically proven to exist (generally).

The organization of the remainder of this paper is as follows.

1) Describe the analytical reasoning and practical implementation of how to transition from one stable oscillation to another.
2) Describe the nonlinear characteristics that govern the speed of transition.
3) Describe the consequences of periodical energy state transitions that apply generally, as well as the significance of Theorem 3 that provides the basis for optimal dynamical energy transitions.
4) Provide a summary and conclusions.

Because of the fact that much of what is presented in not readily apparent in the literature, more details and additional confirming results are shown in the Appendices.

II. Multistable Transitions

In order to develop the arguments which follow, a nonlinear circuit representation for the generalization of dynamics will be pursued. This means that if a system can be represented by an equivalent circuit (which is often the case), then the analysis is applicable to that system.

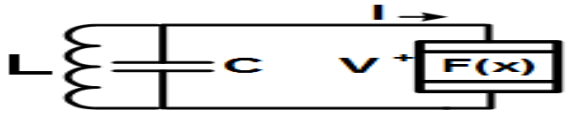

Fig. 1. Nonlinear *RLC* circuit.

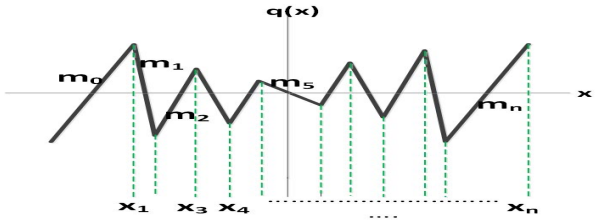

Fig. 2. Generic odd-symmetric continuous PWL function, $f(x)$, comprised of a slopes m_j and breakpoints x_j

Consider the generalized nonlinear RLC circuit shown in Fig. 1, where "R" is actually, $F(x)$, a negative resistance device that is qualitatively described in Fig. 2. Necessarily, there must exist some "internal" energy in order to support "negative resistance." Such a device and implementation were originally reported in the works of Viviani [15], Saet and Viviani [16], [17], and associated references within. Of particular note is the fact that such a system (that is represented by a circuit), with a suitably implemented nonlinearity, $F(x)$, will support more than one stable limit cycle (oscillation).

Theorem 3 indicates that a system that gives rise to multiple stable oscillations can be systematically synthesized. In this work, a simple discrete device implementation is provided.

The class of systems under consideration are described as Lienard Systems of the form

$$\dot{x} = P(x, y) = y - F(\mathbf{x});\ \ \dot{y} = Q(x, y) = -g(x). \qquad (1)$$

Lienard systems are described in several references and are summarized in Perko [18]. Fig. 1 indicates a physical realization for (6). See the Appendix B description of the relationship between $f(x)$ and $F(x)$ for a Lienard-type equation.

For the representation of a general piecewise linear (PWL) function, $F(x)$, the notations and conventions found in Chua and Kang [19] are applied. Refer to Fig. 2 for clarity where the slopes m_j and breakpoints x_j are implicitly defined, without losing generality. In this formulation, some additional general representations associated with discontinuities are omitted as we are concerned strictly with continuously differentiable functions, $F(x)$.

Lemma 1: Resorting to the definitions implied in Fig. 2, any PWL continuously differentiable (denoted as $\mathbf{C}^1$) function $q(x)$ can be represented as follows:

$$q(x) = a_0 + a_1 x + \sum_{j=1}^{n} \{b_j |x - x_j|\};\quad x_1 < x_2 \cdots < x_n$$

$$a_1 = \frac{1}{2}(m_0 + m_n);\quad a_0 = f(0) - \sum_{j=1}^{n} b_j |x_j|$$

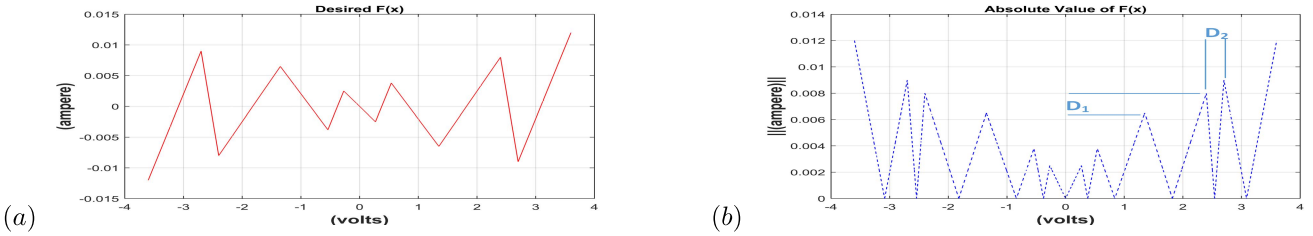

(a) (b)

Fig. 3. (a) Specific $F(x)$ (see Fig. 4 for synthesis details) for the system of Fig. 1 for comparison to (b) |F(x)| (x is a voltage in this case).

$$b_j = \frac{1}{2}(m_j - m_{j-1}), \quad j = 1, 2, \ldots, n. \tag{2}$$

The main result pertains to the nature of PWL nonlinearities, $F_{PWL}(x)$, which can be thought of as a subset of generalized nonlinearities $F(x)$. In this context, $q(x)$ of (2) provides a means for constructing $F(x)$. The subscript is omitted for convenience (the nonlinearity need not be PWL; precise formulations are easier to describe in a PWL format). The idea is to be able to create predetermined and controllable multiple stable equilibriums (limit cycles) for the system of the type shown in Fig. 1. All the proposed electronic systems, and in particular, $F(x)$, adhere to the tenants of *Weierstrass Approximation Theorem* [20] and *Brayton–Moser Theorem* [21].

Definition 2:

$$\mathbb{E} = \{2k : k \in \mathbb{Z}\}; \quad \mathbb{O} = \{k : k \in \mathbb{Z}\}$$

where $\mathbb{E}$ is the set of even integers and $\mathbb{O}$ is the odd integers.

Theorem 3: A system that is described by (6), which contains continuously differentiable $F(x)$, and $g(x) = x$, will always give rise to exactly $\Omega = \frac{n-1}{2}$ limit cycles, Γ_p, $\{\Gamma_p \mid p = 1, 2, \ldots, ((n-1)/2)\}$, when $F(x)$ is described as follows.

1) Following the notations indicated in Lemma 1, for a given continuously differentiable $F(x)$ with $\{m_j \mid j = 0, 1, 2, \ldots, n \in \mathbb{O}\}$, we require that $\{0 < m_j < \infty \mid j \in \mathbb{E}\}$ (including 0) have strictly positive slope and $\{-\infty < m_j < 0 \mid j \in \mathbb{O}\}$ have strictly negative slope.
2) $F(x)$ will have strictly n real roots, with one real root between each break points as described in Lemma 1.
3) $F(x)$ will be odd-symmetric $F(x) = -F(-x)$ $[-\infty < x < \infty]$. See Fig. 3(a) and (b) for a representative example of such a condition.
4) *Most importantly*—the set of nonzero extremes points for $|F(x)|$ will be described by a strictly monotonic increasing function, $x \in \mathbb{R}$. This is clearly illustrated in (for example) Fig. 3(b).
5) $F(x) \to \pm\infty$ as $x \to \pm\infty$.

Moreover, there will be $\frac{\Omega}{2} + 1$ *stable limit cycles that result from such an* $F(x)$.

Remark 4: Unlike the previous results in the literature, these results are not limited to just so-called quasilinear oscillations. They are valid over all ranges of oscillations from quasilinear to relaxational in nature. Llibre *et al.* [22], [23] provides a partial verification of this result. The proof is provided in Appendix D.

III. F(x) Synthesis

The selected method to implement desired nonlinearities is represented in a sequential fashion. Some type of feedback is necessary to acquire negative resistance regions. A suitable means involving (reliable) operational amplifiers (OP-AMPs) is described in Fig. 4 and (3) [24] as follows:

$$\begin{aligned} &R_3 > 0; \quad E_1 = \frac{E_{B1}E_{S+} + E_{B2}|E_{S-}|}{E_{S+} + |E_{S-}| + E_{B1} - E_{B2}} \\ &R_4 = [\frac{E_{B1} + |E_{S-}|}{E_1 - E_{B1}}]R_3; \quad R_7 = \frac{R_3 + R_4}{(m_0 - m_1)R_3} \\ &R_6 = \frac{R_7}{m_0 R_7 - 1}; \quad E_2 = R_6[m_0 E_{B1} + \frac{|E_{S-}|}{R_7} - I_{B1}]. \end{aligned} \tag{3}$$

In (3), $E_{S\pm}$ refers to the supply voltages for the OP-AMP. The other parameters are indicated in Fig. 4.

A. F(x)-Based System Examples

Changing only L or C or both, while retaining the exact same topological nature of the system indicated in Fig. 4, both quasilinear and relaxational multistable devices are realized as a consequence of Theorem 3. This representation is referred to as a virtual quantum well multi-stable oscillator (VQWMO). This is an autonomous system since there are no external forcing functions. The associated steady-state equilibrium conditions are strictly a function of the initial conditions (and the associated domains of attraction). The resultant oscillations are stable (quantized) in terms of both amplitude and frequency. For the single element $F(x)$ case, the frequency (period of oscillation) for all limit cycles is roughly the same.

In order to consider an actual practical realization, some additional insight is appropriate. In particular, it is useful to note that the parameter μ of the Rayleigh form of a Lienard Equation (8) can be derived from the Lieanard form (6) and that $\mu = (L/C)^{1/2}$ for the system in Fig. 1.

For the nonlinearity described in Fig. 4, an actual implementation results in a nonlinearity as described in Fig. 5. It is evident that this nonlinearity will give rise to three stable limit cycles (oscillations) and two unstable ones that are separatrices in the phase plane. The phase plane is equivalent to the I–V characteristic plane for $F(x)$ and this relationship is illustrated in Fig. 6. It is important to note that the means for synthesizing the nonlinearity of Fig. 6, based on two transistors per branch as compared with OP-AMPS, is the simplest possible, as compared to what was shown in Fig. 5. In general, for alternative systems of interest, the nonlinearity need not be synthesized with electronic components. More

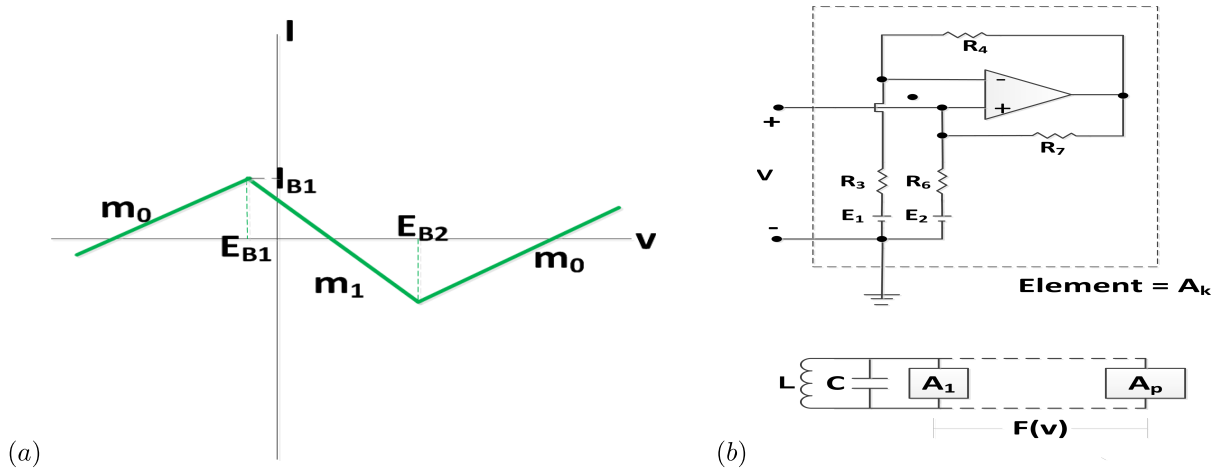

Fig. 4. (a) Indicated PWL characteristic, A_k, consistent with Lemma 1 formulations and is realized by the (b) OP-AMP circuit, for set of parameters specified by (3). The parallel combination of each element, A_k, with suitably determined parameters achieves the desired system associated with Theorem 3 and Fig. 1, for the three stable limit cycle case, $p = 5$, $k = 1, \ldots, p$. Roughly, the associated nonlinearity, $F(x)$, where x is a voltage looks like that shown in Fig. 3(a).

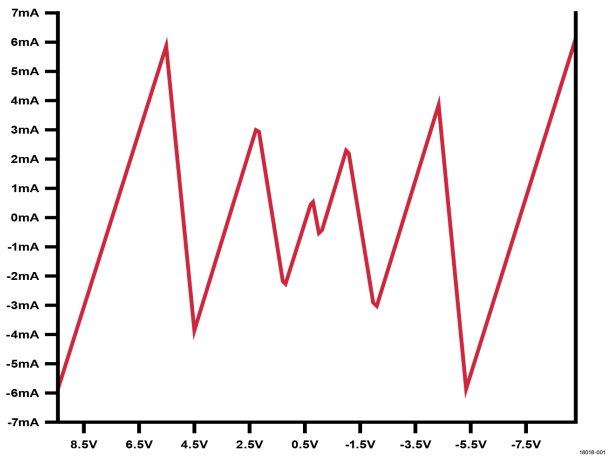

Fig. 5. Synthesized nonlinearity, $F(x)$ by the approach in Fig. 4.

generally, it would be characterized by creating varying electrodynamic boundary conditions with changing permeability and/or dielectric constants. It is also important to note that the nonlinearity need not be PWL. Appendix B shows some results for devices that were realized with a nonlinearity dependent on branches with two transistors. As shown in Appendix B, the resultant waveforms are not as precisely formulated due to the difficulties of working with off-the-shelf transistors. OP-AMPS yield more desirable results when tight tolerances are required and device substrate level implementation is unavailable. These devices are more suitable for illustrating the governing principles.

With the nonlinearity in Fig. 5 applied to the circuit shown in Fig. 1, the resulting stable oscillations are shown in Figs. 7 and 8. The only difference between these two examples is the values of L and C. Hence, as outlined in Theorem 3, both quasilinear (Fig. 7) and relaxation (Fig. 8) oscillations are achieved. With respect to fast switching times, the relaxation oscillations are a prime candidate, as the rise (fall) times are much faster.

B. High Power System Fast Switching Considerations

The previous section demonstrated the practical synthesis considerations for a "low power" situation. For convenience, the circuit shown in Fig. 4 was utilized as the simplest two-transistor formulation for each branch of the system illustrated in Fig. 6 was not available. Specifically, when working with available commercial transistor parts at lower voltages, it is not convenient to realize a suitable $F(x)$. For a high power implementation, a two-transistor per branch approach would be pursued. The two-transistor formulation is also more closely aligned with equivalent circuit nonlinearity considerations associated with a naturally occurring physical system, such as a plasma.

In order to make the transition times as quick as possible, it is clear that the parameter $\mu = (\frac{L}{C})^{\frac{1}{2}}$ is the important governing relationship. In fact, μ is directly related to the Lyapunov Exponents that are an indicator of the rate of convergence to a stable limit cycle [16]. For very large values of μ (theoretically), convergence can become infinitely short. While there are obvious practical limitations, it is noteworthy that this feature is what provides a forcing function that is not available in 1-D solutions. Hence, operating in the 2-D phase space is imperative in order to provide a "force" that directly impacts switching speeds. It is conceivable that one might make this conclusion based purely on first principles. However, this result shows precisely how to receive a desirable result.

C. Pulse Shaping Considerations

While Section III-B may highlight some key characteristics regarding switching speeds, there are further important considerations. Pulse shaping is an important one. Depending upon the value of μ, it is conceivable to create an oscillation that has the desired shape and duration by either biasing the output or else rectifying it. If this were the case, there would not be a need to have more than one stable oscillation and a relaxation oscillation with a nonlinearity, $F(x)$, yielding only one stable solution would suffice. However, if it is desired

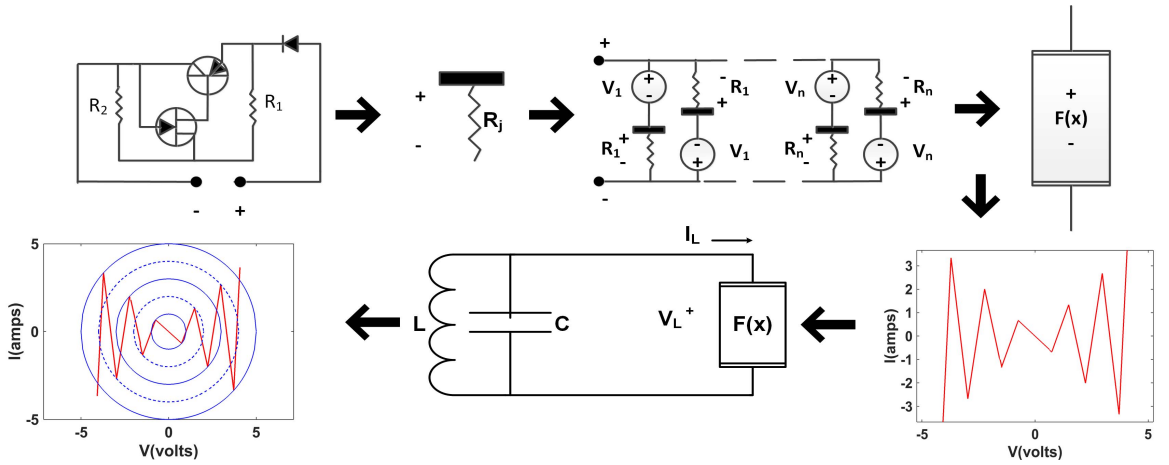

Fig. 6. Multistable device synthesis.

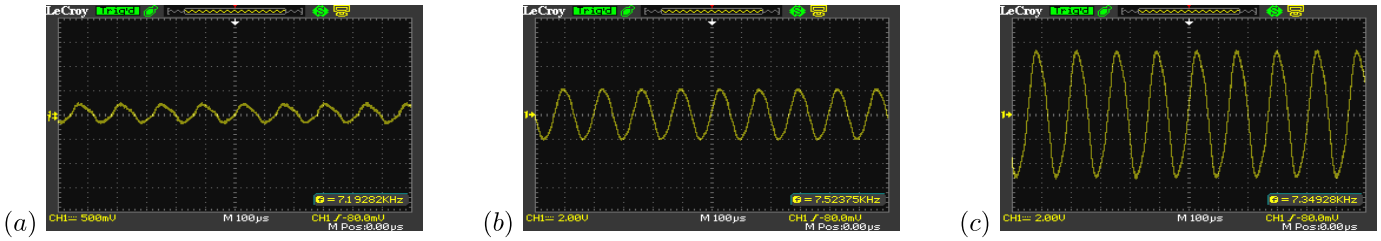

Fig. 7. Time-domain representation of physically realized quasilinear VQWMO with three stable limit cycles. This case is referred to as a quasilinear oscillation where the oscillations are near sinusoidal. In this case, $L = 36$ mH and $C = 0.5\mu$F. This is the small $\mu = (\frac{L}{C})^{\frac{1}{2}}$ case. (a) Smallest limit cycle. (b) Middle limit cycle. (c) Largest limit cycle.

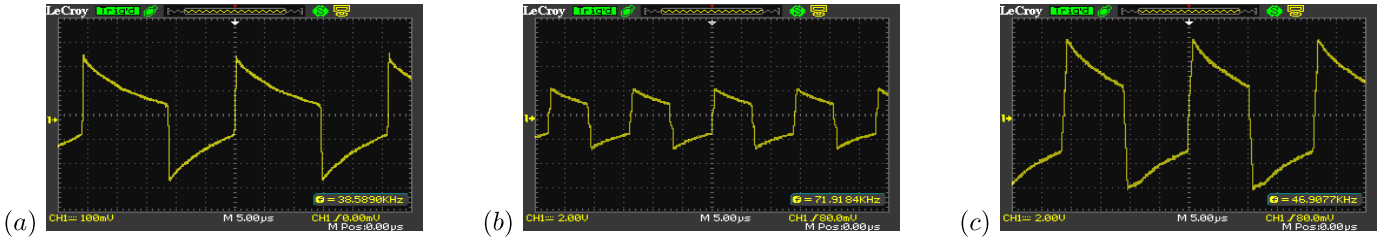

Fig. 8. Time-domain representation of physically realized quasilinear VQWMO with three stable limit cycles. This case is referred to as a relaxation oscillation where the oscillations are far from sinusoidal. In this case, $L = 36$ mH and $C = 0.00005\mu$F. This is the large $\mu = (\frac{L}{C})^{\frac{1}{2}}$ case. Note that the scale is amplified on small oscillation for clarity. (a) Smallest limit cycle. (b) Middle limit cycle. (c) Largest limit cycle.

to further enhance the shape of a high energy pulse, then the VQWMO is uniquely suited to this task. In this work, the general consideration is to transition from one (average) energy to another. If a single stable limit cycle suffices, then this can be viewed as a degenerate "transition," which happens to be consistent with the overall results presented.

It is clear that large oscillations, when there are more than one, are at increasing (average) energy levels. Hence, in order to switch from a low energy output to a high energy one, given the 2-D nature of the phase plane dynamics, it is necessary to implement two discrete changes in initial conditions. A transient voltage applied to the elements of the system in Fig. 1 is all that is necessary. For the systems that have been practically realized, this is easily realized with a simple "one-shot" switch. Alternatively, when speed and precision are important, one can imagine a photosensitive switch activated by a laser. The turn on and off would be consistent with the speed of light. For an initial condition near the first limit cycle (in the domain of attraction of the smallest limit cycle), the smallest limit cycle would result. A second application, near the largest limit cycle, would result in that largest output. A final application of changing initial conditions would be to return to the smallest limit cycle. In this manner, the required "pulse" would result. A simulation for this is shown in Fig. 9. In this scenario, suitably fast convergence to stable equilibrium is assumed. An actual fabricated circuit based on these principles is described in Figs. 11 and 12.

In the particular case of basing switching operations on a particular multistable Lienard-type oscillator, it is apparent that the parameter μ, combined with a suitable nonlinearity and suitable initial conditions, are key factors in determining the rate, shape, and timing of completely controllable pulses that take on desirable characteristics. This approach and associated forcing functions are unavailable by conventional approaches.

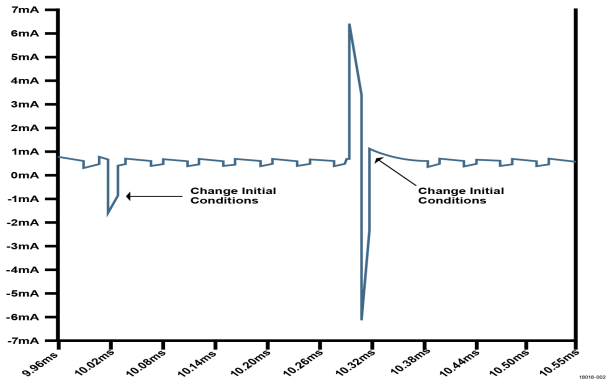

Fig. 9. SPICE simulated pulse shaping for the circuit in Fig. 1 with the nonlinearity in Fig. 5 with L = 1.5 mh and C = 0.000022 μF. Since there are three stable limit cycles (only two are necessary), initial conditions are applied to change oscillation from the small to the large and then back again to the small cycle. By changing the points at which initial conditions are applied, the shape of the pulse can be as narrow as desired—even a portion of a limit cycle for a suitably large μ. Also, note the delay between applying the initial conditions and when the larger oscillations actually began—this may be an artifact of the numerical integration incorporated into SPICE. In this manner, it is straightforward to switch from low power to higher power in a controlled manner.

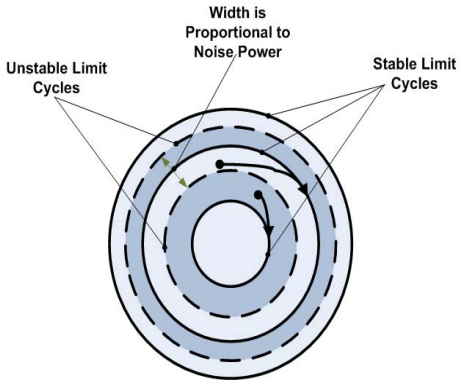

Fig. 10. Phase plane limit cycle convergence details. The phase plane is divided into concentric domains of attraction. Since the limit cycles are periodic, there is an associated zero crossing for both current and voltage. Hence, by applying a zero power voltage or current at the appropriate location in the phase plane, for the desired limit cycle, the transition will take place. The rate of the transition is faster with increasing μ, which, in turn, is proportional to the associated Lyapunov Exponents [16]. Note that as μ increases, the resultant phase plane periodical regimes become less and less elliptical [25].

D. Initial Conditions Power Requirements

Fig. 10 illustrates the requisite details regarding switching from one limit cycle to another. Large power levels are not necessary, as initial conditions can be applied near the zero crossing for the oscillator in order to transition to a new (average) energy level resultant domain of attraction.

Because of the low power requirements, the changes in initial conditions to the oscillator are amenable to making use of a laser with a photosensitive receptor circuit in order to make application to be as precise as desired.

An illustration of these principles is shown in Fig. 11.

E. Further Nonlinearity Considerations

Fig. 3(b) introduces two parameters D_1 and D_2. These parameters are a key to determining the location and boundaries between the multiple domains of attraction. By assuring

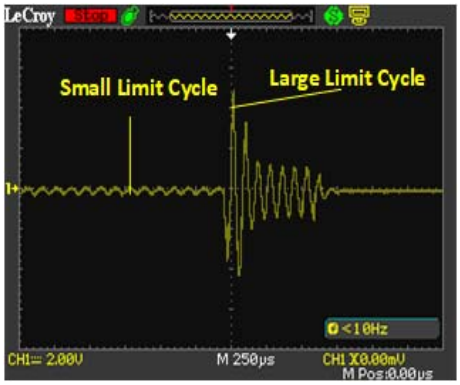

Fig. 11. Oscilloscope trace for actual pulse formation consistent with Figs. 9 and 10. The return to the small limit cycle, in this particular circuit embodiment, was influenced by the middle stable limit cycle, which prolonged the return to the small stable limit cycle. If this had not been present (the actual device has three stable limit cycles), then the return to the small limit cycle would have been faster. The period of time that the device is oscillating on the middle stable limit cycle is consistent with the rate of decay of the change in initial conditions. If there had been just two stable limit cycles, this would have been avoided (and a typical field application would have been designed with this in mind). Some modifications to μ were necessary as compared to the circuits illustrated in Figs. 7 and 8. The nonlinearity, $F(x)$, in all the circuits (oscilloscope traces) is the same and was implemented as described in Fig. 5. Note that the small limit cycle is barely visible in the right side of the oscilloscope trace. The digital oscilloscope was slow to adjust completely. If the oscilloscope is allowed to run continuously, it is clear that the small oscillation is resumed. The deviation from the ideal situation described in Fig. 9 is governed by the parameter μ, the time constant of the applied initial condition, as well as the number of stable limit cycles present. For sufficiently large μ and sufficiently "sharp" initial conditions, the number of limit cycles is irrelevant.

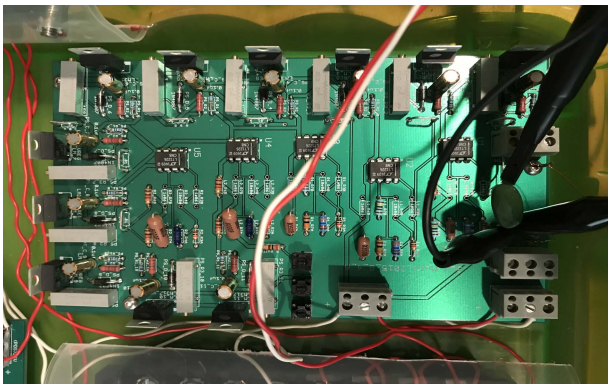

Fig. 12. Printed circuit assembly showing the fabricated results for an actual circuit to realize an $F(x)$ that provides for three stable limit cycles. The nonlinearity is dependent upon the LT 1226 OPAMP as described in Fig. 5.

that they are sufficiently large, it provides for suitable large separation between the average energies of the resultant stable oscillations. These elements of the design represent an additional degree of freedom.

IV. Consequences of Multiple Stable Equilibriums

It is worthwhile to take account of the significance of transitioning from one limit cycle to another. Given that pulse formation is necessarily something that is described in the dynamical phase plane, then only two sorts of stable transitions are possible. Stable equilibriums only come in two sorts, either: 1) limit cycle or 2) fixed point. This implies only

three sorts of transitions are possible: 1) fixed-point-to-fixed-point; 2) fixed-point-to-limit-cycle; or 3) limit-cycle-to-limit-cycle. Clearly, only one of these transitions conforms with a dynamical system that remains a dynamical system. Stability is required for observability (accuracy) and controllability (precision). Engineered systems always rely on these principles.

In the case of a fixed point-to-limit cycle transition, in order for equilibrium to be reached, which signifies a "known" (end-state) condition, the system must transition from being dynamical to rest. Alternatively, it must transition from rest to a dynamical state. In the course of this transition, necessarily, energy must be lost to reduce inertia, or else extra energy must be added to overcome rest-state inertia. This is inefficient in terms of both energy and associated time response. However, in the case of limit-cycle-to-limit-cycle transitions, from one periodical state to another stable periodical state, this has the potential to be more efficient in terms of both energy and time of transition. This can alternatively be interpreted as continuously dynamical without inefficiency. Hence, such an approach can be more efficient with respect to creating 2-D energy transitions in the phase plane. For a suitably designed system, the inefficiencies of transitioning to (or from) a rest state can be avoided. This is a very significant observation as it suggests that the key to efficient energy transitions, regardless of the medium (HPM, lasers, or else plasmas) are best achieved by a suitable nonlinearity, which allows for transitions from one periodical solution to another. This does not appear to be generally known or understood. The nonlinearity described by Theorem 3 may not be the only one that allows for limit-cycle-to-limit-cycle transitions in the phase plane, but it is certainly representative of one that can be physically realized to achieve such efficiencies.

V. Conclusion

A nonlinear oscillator with the following characteristics:

1) multiple stable limit cycles;
2) simple parameter that allows for determining the quasi-linear or else relaxational nature of the oscillations;
3) simple means to transition from one energy level to another.

provides the basis for realizing virtually any desired pulse characteristic in the phase plane. As there is an inherent forcing function (in this case it is not external) associated with an oscillator and there are associated Lyapunov Exponents that govern convergence to solutions [16], an oscillator is an ideal means in order to create suitably fast transitions. Assuming sufficiently large Lyapunov Exponents are chosen, then the multistable oscillator presented will allow for as fast as desired transitions from one energy level to another, in a bidirectional manner. By choosing one stable limit cycle to be at low energy level and another at high energy level, the basis for a rapid bidirectional switching transition is created. Such an approach is suitable for a variety of applications, especially those requiring pulse shaping in order to maximize power delivery with minimal energy.

As is shown in the analysis, as well as the associated physics, an oscillator of any sort requires a "negative resistance." The special form of a nonlinear resistor that provides for multiple zones of negative resistance is a particularly important result. As the associated mathematics indicate such a nonlinearity will be a prerequisite of 2-D pulse shaping for a variety of applications across the spectrum of pulse shaping requirements, including high power situations.

Appendix A describes why it is feasible to represent any pattern of interest based on phase plane (only) considerations. This basis underlies the generality of the results presented in this paper. Appendix B provides more insight into the nature of the governing mathematics and physics associated with the VQWMO.

Appendix A
Topological Considerations

Imagine that the device is going to be useful in representing systems or objects that are defined in what can equivalently be thought of as four dimensions, time and space, or more formally as a Minkowski Space.

Theorem 1: For an invariant dynamical system in a Minkowski Space, a fixed symmetric pattern is represented by no more than two complex planes (manifolds), $\mathbb{C}^2$.

Proof: The Cayley–Dickson formulation [26] assures that it is possible to successively create sequences of Algebras, such that the next is twice the dimensionality of the previous one. For our purpose, it is assumed that all that we would like to "recognize" is defined by Minkowski Space, which is a fourth-order space covered by Cayley–Dickson [26] and generally attributed to Hamilton. It is, therefore, possible to show that for the generalized quaternion

$$q = w + x\mathbf{i} + y\mathbf{j} + z\mathbf{k}$$

where $\mathbf{i}$, $\mathbf{j}$, $\mathbf{k}$ are mutually perpendicular bivectors, which satisfy the relationship $\mathbf{i}^2 = \mathbf{j}^2 = \mathbf{k}^2 = \mathbf{ijk} = -1$, and $w, x, y, z \in \mathbb{R}$, then

$$q \equiv (w + x\mathbf{i}) + (y + z\mathbf{i})\mathbf{j}$$

represents two independent manifolds in $\mathbb{C}^2$, which are sufficient to represent the space. Further details can be found in [27].

Next, we recognize that by choosing the two complex planes to be orthogonal, with one of them perpendicular to the time-varying flow of the system, then only one manifold in $\mathbb{C}^2$ is sufficient to represent a system that is stationary.

Finally, since according to the Noether Theorem (assuming we have a suitably constructed system we wish to represent), [28] then we can be assured that a suitably conservative system will give rise to a stable symmetric pattern in the indicated plane(s). ■

Remark 1: The concept of using planar projections to represent patterns of interest is well founded for generalized dynamical systems of the natural world.

Appendix B
Multistable Devices

For simplicity, it will be assumed that the periodic signals of interest are representable in the complex plane $\mathbb{C}^n$, where $n = 2$.

If the signal of interest, $s(t)$, is periodic and is representable in the phase plane $\mathbb{C}^2$, then one can imagine that it must correspond to a closed orbit. Since more typically, $s(t) = f(t)+\eta(t)$ where $f(t)$ is the actual signal with additive noise, $\eta(t)$, it is important to consider that for practical situations, $s(t)$ will have a noise component that will not detract from its ability to remain periodic.

The classical nonlinear system, especially with respect to dynamics on a particular manifold of interest is the subject of various well-established works [3]–[7], [18]. The "dot" operator indicates a derivative with respect to an independent parameter of time for the classical nonlinear system

$$\dot{\mathbf{x}} = \mathbf{f}(\mathbf{x}).$$

In general, $\mathbf{x} \in \mathbf{R}^n$. It is often convenient to represent planar systems, where $n = 2$, as

$$\dot{x} = P(x, y); \quad \dot{y} = Q(x, y). \tag{4}$$

In some cases, the general nonlinear system can be parameterized to be dependent upon a scalar quantity, $\mu \in \mathbf{R}$, which can be thought of as

$$\dot{\mathbf{x}} = \mathbf{f}(\mathbf{x}, \mu) \tag{5}$$

and the parameter μ is a so-called bifurcational parameter; very often as this parameter is allowed to vary, the phase-portrait, or else the generalized solutions of the systems of equations, ϕ_t, take on qualitatively different topologies depending upon this parameter.

With this in mind, the class of systems under consideration is described as Lienard Systems of the form

$$\dot{x} = P(x, y) = y - F(\mathbf{x}); \ \dot{y} = Q(x, y) = -g(x). \tag{6}$$

Such systems are described in many references. As shown in [18], the following parameters will also be of use:

$$\mu F(\mathbf{x}) = \int_0^x \mu f(s)ds; \ G(x) = \int_0^x g(s)ds \tag{7}$$

where it is well understood that (6) is equivalent to the autonomous system

$$\ddot{x} + \mu f(x)\dot{x} - g(x) = 0. \tag{8}$$

One of the best known examples of such a system is the van der Pol Oscillator, which is a particular version of a Lienard system

$$\ddot{x} + \mu(x^2 - 1)\dot{x} + x = 0. \tag{9}$$

Equation (9) is known to give rise to a single limit cycle (oscillation), which is characterized by a closed continuous curve in the phase plane. As the parameter $\mu \to 0$, the limit cycle becomes more and more circular, as compared with the so-called relaxational oscillations that occur when $\mu \to \infty$.

For convenience, a limit cycle associated with a generic nonlinear oscillator will be defined by the symbol Γ where the time-varying nature of the limit cycle is implicitly assumed, as such a limit cycle is periodic by definition. The associated planar flows for such a nonlinear oscillator are represented by $\phi_t(\mathbf{x_0})$, where $\mathbf{x_0} = (x_0, y_0)$ are the associated planar initial conditions. The time-varying nature of the flow is explicitly indicated, as unlike the limit cycle, Γ, the nature of the flow will depend upon the initial conditions. For simplicity initially, the possibility of multiple different limit cycles is neglected.

The limit cycle, Γ, for (9) is centered with respect to the origin that is termed a center. The planar flows associated with the initial conditions $\mathbf{x_0} = (x_0, y_0)$ are such that $|\mathbf{x_0}| = \Gamma^- < |\Gamma|$, so that $\phi_t(\mathbf{x_0})$ will evolve over time to a steady state limit cycle such that $|\Gamma| = 2$ (for sufficiently small μ). We only assume sufficiently small μ, but the same is true for larger μ under suitable circumstances [25]. Similarly, for initial conditions outside of these steady-state conditions, Γ, the associated planar flow when $|\mathbf{x_0}| = \Gamma^+ > |\Gamma|$, $\phi_t(\mathbf{x_0})$ will end up in the same steady-state oscillation, Γ. As the parameter μ is increased, the shape of the oscillations will become less and less sinusoidal, which means that $|\Gamma| = K(t) \neq 2$, where K(t) represents the time-varying nature of the magnitude $|\Gamma|$ resulting for $\mu \gg 0$. While the nature of (9) looks disarmingly simple, the nature of the solutions is particularly rich. It is important to indicate that not all variations of (6) will give rise to steady-state stable oscillations. This means that certain conditions on F(**x**) (or equivalently f(**x**)) and G(**x**) [or equivalently g(**x**)] will be the primary means by which the character of the phase plane portrait will be determined.

As first exploited in the works of Viviani and Saet [15]–[17], [25], [29]–[33] of particular interest is the occurrence of more than one limit cycle associated with the system (6).

In this regard, citing a particular Theorem [18] is useful for illuminating the character of these limit cycles for small parameter μ [realizing that (5), which is dependent upon μ can be subsumed in (6) and, therefore, takes on the formulation indicated in the following proof].

Theorem 2: For $\epsilon \neq 0$ sufficiently small, the Lienard system (6) with $g(x) = x$ and $F(\mathbf{x}) = \epsilon[a_1x + a_2x^2 + \cdots + a_{2m+1}x^{2m+1}]$ has at most m limit cycles; furthermore, for $\epsilon \neq 0$ sufficiently small, this system has exactly m hyperbolic limit cycles that are asymptotic to the circles of radius r_j, $j = 1, \ldots, m$, centered at the origin as $\epsilon \to 0$ iff the mth degree equation

$$\frac{a_1}{2} + \frac{3a_3}{8}\rho + \frac{5a_5}{16}\rho^2 + \frac{35a_7}{128}\rho^3 + \ldots + \binom{2m+2}{m+1}\frac{a_{2m+1}}{2^{2m+2}}\rho^m = 0$$

has m positive roots $\rho = r_j^2$, $j = 1, \ldots, m$.

Proof: See Blows and Perko [34], Theorems 1.1–1.3, and Proposition 1.1. ■

Remark 2: Similar results are found in Andronov *et al.* [5]—Theorem 76 and other results [17]. In addition, it is important to note that the "center" at the origin when associated with more than one hyperbolic limit cycle can either be stable or unstable depending upon the number of roots of the equation in Theorem 2. Also, as a result of Green's Theorem on the plane, the "nested" limit cycles (when there is more than one) must alternatively be stable and unstable, with the unstable ones serving as separatrices for the domains of attraction for the stable ones. Finally, Theorem 2 addresses the

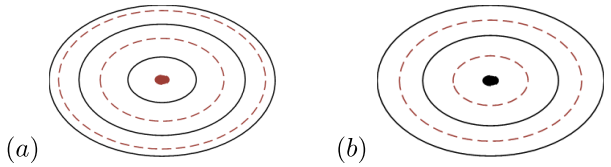

Fig. 13. (a) N+1 order phase plane portrait and the associated partitioning of stable (black) and unstable (red) limit cycles of the phase plane. (b) Nth order (versus N+1) partitioning of the phase space in a complementary manner.

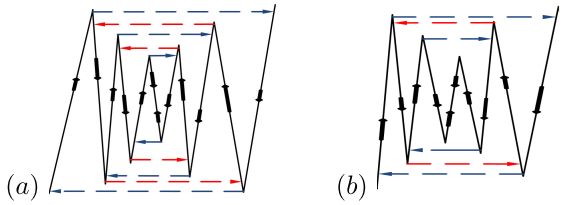

Fig. 14. (a) and (b) represent the nonlinearities that correspond to Fig. 13 (a) and (b), respectively. The superimposed flows illustrate the approximate location of limit cycles for $\mu \gg 1$ in (6) (nonlinearity is only the solid portion of the curve, which is represented in the phase plane, as in the case in Fig. 13).

situation of a small parameter variation from a linear case. In the event that $\mu \to \infty$, it is necessary to resort to other means to determine the nature of the associated limit cycles [35]. The nonlinearities presented in this work are also valid for large μ, and a proof results by combining Mishchenko and Rozov [35] and Hirsch and Smale [36] results.

Based on Theorem 2, it is, therefore, completely reasonable to expect to partition the phase plane as shown in Fig. 13. As μ increases and the associated oscillations become more and more relaxational, the character of the limit cycles will adhere more closely to the dotted lines indicated in Fig. 14 [35]. Fig. 17 illustrates the interdependence of the nonlinearity $F(\mathbf{x})$ and the associated limit cycles for an actual device for intermediate μ.

Appendix C
Physical Device Realization—Virtual Quantum Well Multi-State Oscillator

The device realization is based on the superposition of multiple negative resistance elements, which are, in turn, combined in parallel (for the case of voltage controlled devices). The result is termed a VQWMO as illustrated in Figs. 6 and 15.

Applying the transmission line equivalent solutions to the Schroedinger Equation [37] and the I–V descriptions suggested in Figs. 6, 14, and 17, what follows represents a discrete component realization of a quantum well multi-state oscillator [38].

The salient feature of (6), F(**x**), is realized by the one-port in Fig. 15. Such a structure can be made to function with discrete components, and other implementations are feasible as well. This structure was first described by Saet and Viviani [32], where there are pairs of identical branches, except for polarity. The representative topological structure of the nonlinear $R_i's$ in Fig. 15 is shown in Fig. 18.

When this structure is combined with suitable inductance and capacitance as illustrated in Fig. 6, this will result in a VQWMO.

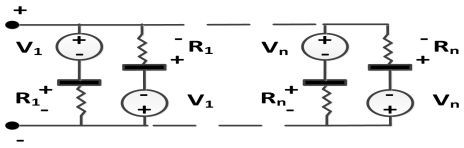

Fig. 15. VQWMO nonlinearity, F(**x**), topological structure.

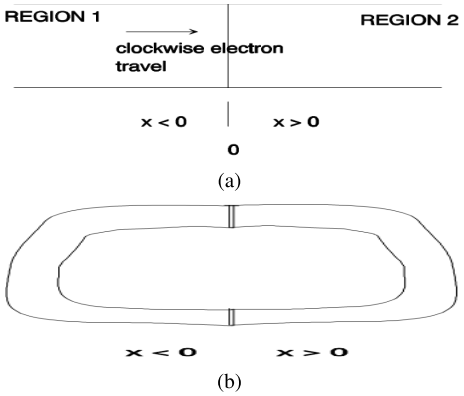

Fig. 16. (a) Infinite source of electrons impinging on a generalized boundary, which may be "transparent." (b) Manner in which such electrons are "contained."

Assuming a clockwise flow of electrons based on a superposition of multiple 1-D components that comprise the multiple nonlinear resistors in Figs. 15 and 6, one can imagine a model that conforms to Fig. 16 associated with the multiple limit cycles previously characterized in Figs. 13 and 14, which are guaranteed by the associated mathematical formulations of the previous section.

1) In terms of the proposed device characteristics in a quantum mechanical sense, a stationary probability density current [37], [39] $\Leftrightarrow$ a stationary average power, where the term power is associated with the product of voltages and currents. This can be derived as follows, assuming sinusoidal variations only in the "x" direction, where Fig. 16(b) suggests a "channel" within which only variations in x are perceptible to a particle

$$S = \frac{\hbar}{2jm^*}\left(\psi^* \frac{d\psi}{dx} - \frac{d\psi^*}{dx}\right) = \frac{1}{2}\mathrm{Re}[\phi\psi^*] = \frac{1}{2}\mathrm{Re}[VI^*] \tag{10}$$

where

a) S $\stackrel{\text{def}}{=}$ probability density current;
b) $\psi^*(x) \stackrel{\text{def}}{=}$ complex quantum mechanical wave function with only x variations;
c) $\phi^*(x) \stackrel{\text{def}}{=} \frac{\hbar}{2jm^*}\psi^* \frac{d\psi}{dx}$;
d) $\hbar \stackrel{\text{def}}{=}$ modified Planck's constant;
e) m* $\stackrel{\text{def}}{=}$ effective mass;
f) j $\stackrel{\text{def}}{=} \sqrt{-1}$;
g) V(x) $\stackrel{\text{def}}{=}$ complex voltage in the x-direction;
h) I(x) $\stackrel{\text{def}}{=}$ complex current in the x-direction;
i) * $\stackrel{\text{def}}{=}$ complex conjugate (generally).

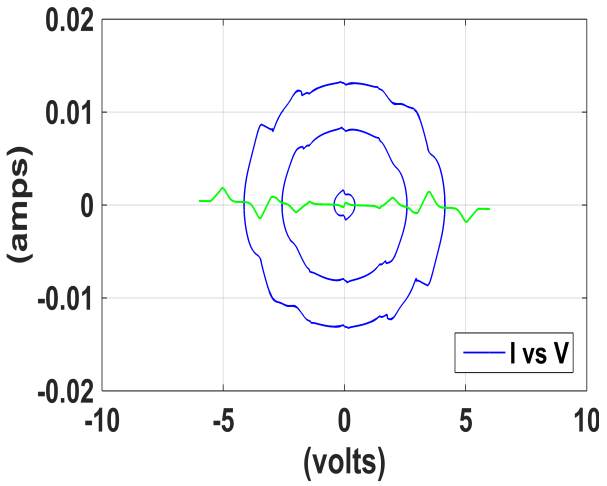

Fig. 17. Phase plane with superimposed characteristic, F(**x**), for Fig. 15 with $N = 6$, based on the nonlinearity in Fig. 18—the profile of voltages is as follows (volts): $V_1 = 3.0$, $V_2 4 = 5.5$, $V_3 = 1.0$, $V_4 = 4.0$, $V_5 = 0.5$, $V_6 = 2.0$; $L = 800$ mH, and $C = 5\mu$ f. The set of resistors is not shown (for simplicity).

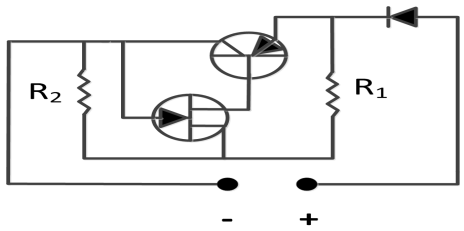

Fig. 18. Nonlinear Elements for each Branch in Fig. 15. Here the FET is 2N4338 type and the bipolar junction transistor (BJT) is a type 2N2905A. The resistor values are somewhat variable per stage but typically in the 50K ohm range.

Hence, we require a device capable of delivering multiple "quantized" power levels, with a finite source of energy.

2) With respect to understanding the function of the proposed quantum mechanical device, losses in the "channels" described in Fig. 16 are essentially nil.

The device proposed in Figs. 6 and 15 is consistent with the indicated solution to the indicated transmission line formulation of the Schroedinger Equation.

The key feature of a VQWMO is the nonlinearity, F(**x**) [or equivalently $f(x)$] of (6). Fig. 17 shows what the combination of superimposing Figs. 13 and 14 looks like for the particular, F(**x**), for Fig. 6. In addition, photographs of physically realized limit cycles are shown in Fig. 19 in order to confirm physical reality of such devices.

Appendix D
Proof of Theorem 3

Lemma 5 (Weierstrass Approximation Theorem [20]): Suppose $\mathcal{F}$ is a continuous real-valued function defined on the real interval $[a, b]$. For every $\epsilon > 0$, there exists a polynomial $p(\mathbf{x})$ such that for all $\mathbf{x}$ in $[a, b]$, we have $|\mathcal{F}(\mathbf{x}) - p(\mathbf{x})| < \epsilon$, or equivalently, the supremum norm $||\mathcal{F} - p|| < \epsilon$.

Remark 6: It should also be noted that the fundamental theorem of Algebra indicates that a polynomial of degree "n" necessarily has "n" roots, some of which may be degenerate. In addition, it is well known that a polynomial can be realized by factoring it in terms of its roots. We will use this to show that for a given PWL function, $f(x)$, a suitable polynomial approximation exists.

Lemma 7 (Brayton–Moser Theorem [21]): Suppose we consider a standard electrical network (the complete details of the term "standard" are omitted for simplicity, but may be better understood by reference to standard texts on circuit theory) of components that are interconnected in a manner that can be defined by a graph $\mathcal{G}$, which is comprised of directed branch currents i_k, and nodal voltages v_k where k indicates the k^{th} branch or node, respectively. Therefore, the set of branch currents for the network can be denoted as the vector **i** and similarly nodal voltages are represented by vector **v**. Hence, the network power, $\mathcal{P}$, can be denoted by the scalar product $\mathcal{P} = \langle \mathbf{v}, \mathbf{i} \rangle$.

Continuing in the spirit of [40] and [41] and recognizing that the generalized network includes nonlinear, possibly time-varying inductors, capacitors, and resistors (to include negative resistance as well), the following definitions are necessary to interpret the final result. Note that further details regarding the exact means to construct the so-called mixed potential function $\mathcal{Q}$ will be omitted for simplicity.

Hence, a differential relationship for the scalar $\mathcal{P}$ can be defined as

$$d\mathcal{P} = d\mathcal{G} + d\mathcal{J}$$

where

$$d\mathcal{G} = \langle \mathbf{i}, d\mathbf{v} \rangle, \quad d\mathcal{J} = \langle \mathbf{v}, d\mathbf{i} \rangle.$$

For completeness, it is useful to recognize that the set of network capacitors and inductors gives rise to matrices **C** and **L**, which are derived from associated graph theory consistent with the vectors **v** and **i**. Furthermore, it is important to note that, in general all elements of the state of the system will be time varying. Hence,

$$\mathbf{i} = \mathbf{C}(\mathbf{v})\frac{d\mathbf{v}}{dt}, \quad \mathbf{v} = \mathbf{L}(\mathbf{i})\frac{d\mathbf{i}}{dt}.$$

Next, we note that the state space is governed by a manifold $\Sigma \subset \mathbb{R}^2 \times \mathbb{R}^2$ that is reduced from a dimension of 3 as a consequence of the fact of the following main result of the Brayton–Moser Theorem:

$$\psi = \begin{pmatrix} \mathbf{i} \\ \mathbf{v} \end{pmatrix}; \qquad \mathcal{Q}(\psi) = \begin{pmatrix} \mathbf{L}(\mathbf{i}) & 0 \\ 0 & -\mathbf{C}(\mathbf{v}) \end{pmatrix}$$

then

$$\mathcal{Q}(\psi)\frac{d\psi}{dt} = \frac{\partial \mathcal{Q}(\psi)}{\partial \psi}. \tag{11}$$

Observations of consequence to what follows.

1) The integral of any curvilinear curve in the state space (phase plane) for each of the quantities $d\mathcal{G}$ and $d\mathcal{J}$ is zero. While the system is dissipative, if the time-varying nature of the system is not constant, then it

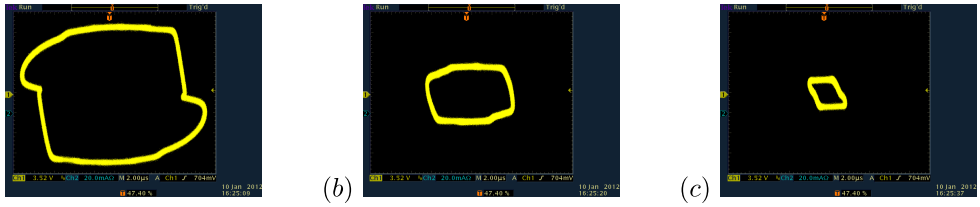

Fig. 19. Physically realized VQWMO with 3 stable limit cycles that are topologically consistent with SPICE simulations shown in Fig. 17. These were realized with different components, with different operational ranges.

must be periodic, assuming it is stable. If the state of the system as determined by $\mathbf{i}$ and $\mathbf{v}$ is periodic, so must be the mixed potential function $\mathcal{Q}(\mathbf{i}, \mathbf{v})$. But since $\mathcal{Q}$ is a measure of "power," then its integral over a curvilinear curve must be zero (indicating something is consuming energy and something is supplying energy in a compensating manner).

2) These observations are valid for whatever nonlinear resistor may exist in the network [40]. This is determinable by relying solely on the inductor and capacitor states. It is valid even if for nonconstant inductors and capacitors.
3) Details of constructing mixed potential functions $\mathcal{Q}$ are consistent with standard circuit analysis methods associated with Kirchoff voltage–current relationships, but they require systematic procedures that are specific network dependent. A simplified example is provided in [40]. In general, simplified examples are not widely seen. For what follows, we are primarily interested in the confirmation that such a function exists, and the details will not be necessary in order to draw conclusions.

All the proposed electronic circuits, and in particular, $F(x)$, adhere to the tenants of *Weierstrass Approximation Theorem [20]* and *Brayton–Moser Theorem* [21].

Lemma 8: As specified in (6) for $g(x) \stackrel{\text{def}}{=} x$, and a particular three-segment $F(x)$ described as in (2) and Fig. 20 by

$$\begin{aligned} F(x) &= \{b_1|x - x_1| + b_2|x - x_2|\} \\ &\qquad x_1 < x_2 \quad \forall \quad |x_1| = x_2 > 0 \\ m_0 &= m_2 > 0 \quad \textit{and} \quad m_1 < 0 \\ b_j &= \frac{1}{2}(m_j - m_{j-1}), \ j = 1, 2. \end{aligned} \tag{12}$$

Such a system can be thought of as a PWL van der Pol Oscillator. In addition, if it is not already obvious, we require that:

1) $F(x)$ will be odd-symmetric such that $F(x) = -F(-x) \ \forall \ [-\infty < x < \infty]$;
2) $F(x) \to \stackrel{+}{-}\infty$ as $x \to \stackrel{+}{-}\infty$.

Such a system will have one unique limit cycle.

Proof: Following from [36, pp. 217–225], we define the regions indicated on Fig. 20 as

$$\begin{aligned} v^+ &= \{(x, y) \mid y > 0, x = 0\} \\ g^+ &= \{(x, y) \mid x > 0, y = F(x)\} \\ v^- &= \{(x, y) \mid y < 0, x = 0\} \\ g^- &= \{(x, y) \mid x < 0, y = F(x)\}. \end{aligned}$$

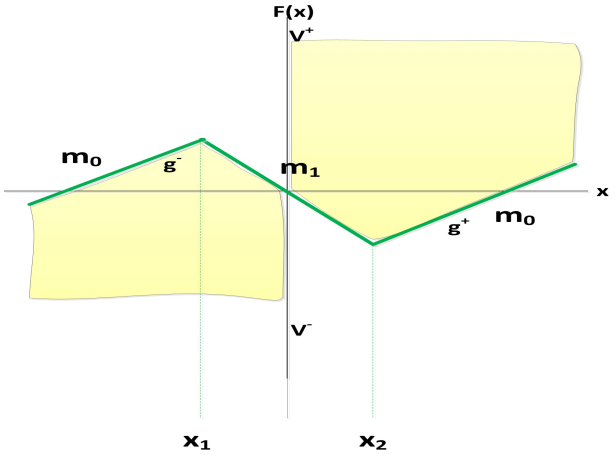

Fig. 20. Specific PWL van der Pol nonlinearity, $F(x)$, and regions proposed in [36].

In [36], instead of $F(x)$, the specific form of the van der Pol Oscillator, $F_{\text{specific}}(x) = x^3 - x$ is declared for the boundaries on the regions of interest. The nature of the associated vector flows, in the vicinity of regions of interest, subject to the indicated boundaries is the key concern. The formulation of the (unlabeled) proof shown in [36] requires only that $F(x)$ is an odd symmetric function, and for each of the indicated regions it is monotonic. Additional conditions mentioned above are also satisfied. Hence, the specific nonlinearity of (12) is topologically equivalent to $F_{\text{specific}}(x)$ described in the van der Pol Oscillator. Therefore, as in the case of the van der Pol oscillator, the so-called proposed PWL van der Pol Oscillator also has one unique limit cycle. ■

Remark 9: These results can also be confirmed independently in [22] and [23].

Remark 10: The formulation presented in [36] will be additionally utilized in what follows. Although not specifically mentioned in [36], for the regions described in Fig. 20, you can think of an additional set of boundaries associated with upper (lower) limits on the indicated ones. In the case of Fig. 20, the additional upper (lower) limits are $\stackrel{+}{-}\infty$.

Proof: To begin, for concreteness, we note that according to Theorem 2, multiple limit cycles for (6), with continuously differentiable polynomials, $\epsilon F(x)_{\text{Theorem 2}}$, and $g(x) = x$, exist. However, the conditions on both ϵ as well the associated coefficients described by Theorem 2 are not sufficient for our purposes. Hence, by application of Lemma 5 and taking note of the fact that any polynomial can be factored dependent upon its roots, we can conclude that $F(x)$ is completely representable by a nth order polynomial. Moreover, it will be

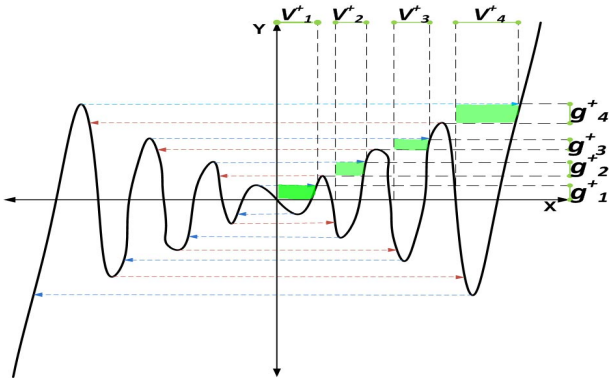

Fig. 21. Critical regions of interest consistent with the formulation of the Theorem on [36, p. 218] in order to extend the proof to multiple limit cycles for a nominal characteristic, $F(x)$. To reduce clutter, only v_k^+ and g_k^+ regions are indicated.

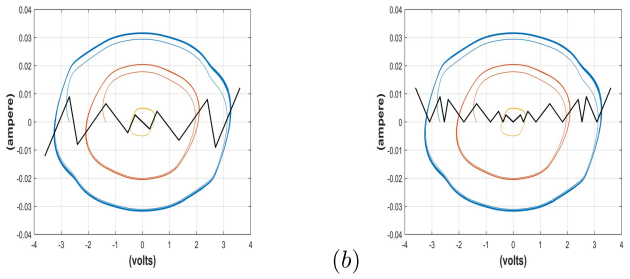

Fig. 22. A specific $F(x)$ for the circuit of Fig. 1, with L = 2.5mhenries and C = 0.22μfarads, is superimposed on the resultant 3 stable limit cycle solutions in (a) versus superimposing |F(x)| on the same result in (b). This is done to show the relationship of the associated dynamical solutions to the generative nonlinearity, $F(x)$ (where x is a voltage in this case).

topologically equivalent in terms of the number of maximums, minimums, and roots. Hence, the PWL representation is not restrictive in nature, as compared with other results. By starting with a PWL representation, an nth order polynomial can be determined, at least some of the time, according to Lemma 5.

Next, we note that according to Lemma 7, if multiple limit cycles exist for Fig. 1 which is one-to-one with (6), then they necessarily will have a mixed potential function $\mathcal{Q}$ according to (11) which will result in concentric curvilinear curves in the phase plane. This is also seen as a consequence of Green's Theorem in the plane. Accordingly, due to Green's Theorem, the limit cycles, with separated concentric $\mathcal{Q}$, will correspond to alternating stable and unstable limit cycles. Moreover, the unstable limit cycles will serve as separatrices (boundaries between) alternating stable and unstable limit cycles. Hence, they can be seen as boundaries on concentric domains of attraction. Presumably, the unstable limit cycles would not be recognizable according to (11), unless an appropriate sign reversal was incorporated into the analysis.

For the next logical arguments, the reader may find it useful to refer to Figs. 3 and 22 as they are the representative of generally arising attributes that are described next. We note that according to Lemma 7, the mixed-potential function has units of power and that it simultaneously must satisfy $F(x)$ (where x is a voltage). Hence, in Fig. 22(b), where $|F(x)|$ is proportional to "energy" in the system, which is dissipative for (6), then the stable solutions must correspond to a negative sloping segment in the right-half-phase plane for $|F(x)|$ and (odd-symmetric) positive-sloping left-half-phase-plane equivalent for $x < 0$. Of consequence is the fact that there exist only a specific set of PWL segments where this can occur. By inspection, the list of candidate locations is obvious. These dependencies related to energy arguments are also evident in Fig. 22(a). However, by referring to Fig. 22(b), it is clear that there are successive local minimums in energy that result from the specific nature of the required $F(x)$. Such a condition is necessary and sufficient for the existence of multiple equilibriums in a circuit (equation), which is governed by (11).

In Lemma 8, the arguments to prove the existence of the van der Pol Oscillator limit cycle first presented in [36] were applied to a single limit cycle PWL case. These are now expanded to consider a multiple limit cycle situation. The reader is referred to Fig. 21, where the arguments on boundaries and flows within regions are expanded and the notations are extended from those of Lemma 8 in an enumerated manner. Assuming that multiple limit cycles exist, then according to Green's Theorem, the boundaries of the zones of attraction must be associated with intervening unstable limit cycles. These unstable limit cycles can be considered to be equivalent in effect to the boundaries of the flows in the phase plane described in Lemma 8 and [36]. That is, the unstable focus at the origin in [36] and Fig. 20 can be represented as an unstable limit cycle (lower) boundary as suggested in Fig. 21. Similarly, an unstable limit cycle (upper) boundary can replace the one at ∞ for Lemma 8, when applied to the case of more than one stable limit cycle. Taking simultaneous account of the restrictions due to Green's Theorem and those of Lemma 7, it is evident that there are specific positive sloping line segments to which the corresponding arguments suggested in Fig. 21, and those of Lemma 8, are applicable. That is, the indicated combination of conditions can only be simultaneously satisfied when the solution to the system impinges on particular segments of the function, $F(x)$. They are determinable by inspection, for any n, for any suitable $F(x)$ consistent with what is proposed.

Therefore, by applying Theorem 2 combined with Lemma 5, it is confirmed that, indeed, multiple limit cycles are feasible, in a specific number, for the specified $F(x)$. By simultaneously applying Lemma 7 and Green's Theorem, the relative locations and number are confirmed by extending the logical arguments of Lemma 8 and [36]. These results are valid for any n. Moreover, unlike the results of Theorem 2, they are not dependent upon a small parameter. ■

Remark 11: These results can be independently confirmed by resorting to arguments described, for example, in [35] as they pertain to relaxation oscillations. As compared with the results pertaining to small parameter variations, the ratio of $(\frac{L}{C})^{\frac{1}{2}}$, for the circuit shown in Fig. 1 governs the nature of the range of possible solutions. Small parameters oscillations are termed quasilinear. As the small parameter grows, the resultant oscillations are termed relaxational. The conditions on $F(x)$ considered in Theorem 3 are invariant with respect to small parameter variations. The topological nature of $F(x)$ is invariant with respect to a small parameter. Hence, the solutions are valid over a wide range. However, there will be obvious

"circuit component" (system related) limitations that will determine the actual range of potential limit cycle variations.

Remark 12: Unlike previous results in the literature, these results are valid for BOTH so-called quasilinear AND relaxational oscillations. These limit cycles are easy to prescribe and determine, which is also confirmed with SPICE. The interested reader can investigate Llibre *et al.* [22], [23] for at least partial verification of the result.

REFERENCES

[1] Z. Liu, H. Huang, X. Jin, and L. Lei, "Design of an X-band gigawatt multibeam relativistic klystron amplifier," *IEEE Trans. Plasma Sci.*, vol. 42, no. 10, pp. 3419–3422, Oct. 2014.

[2] J. C. Martin, "Nanosecond pulse techniques," *Proc. IEEE*, vol. 80, no. 6, pp. 934–945, Jun. 1992.

[3] H. Poincaré, "Mémoire sur les courbes définies par une équation différentielle," *J. Mathématiques*, vol. 7, pp. 375–422, 1881.

[4] A. A. Andronov, E. A. Leontovich, I. I. Gordon, A. G. Maier, and A. G. Maier, *Theory of Second Order Dynamical Systems*. New York, NJ, USA: Wiley, 1973.

[5] A. A. Andronov, E. A. Leontovich, I. I. Gordon, and A. G. Maier, *Theory of Bifurcations of Dynamic Systems on a Plane*. Jerusalem, Israel: Israel Program for Scientific Translations, 1971.

[6] J. Guckenheimer and P. Holmes, *Nonlinear Oscillations, Dynamical Systems, and Bifurcations of Vector Fields*. New York, NY, USA: Springer-Verlag, 1983.

[7] S. S. Sastry, *Nonlinear Systems*. Springer-Verlag, 2010.

[8] Y. Gao, Y. Li, and J. Zhang, "Invariant tori of nonlinear Schrödinger equation," *J. Differ. Equ.*, vol. 246, no. 8, pp. 3296–3331, 2009. [Online]. Available: http://www.sciencedirect.com/science/article/pii/S0022039609000412

[9] V. G. Veselago, "The electrodynamics of substances with simultaneously negative values of ϵ and μ," *Soviet Phys. Uspekhi*, vol. 10, no. 4, pp. 509–514, 1968. [Online]. Available: http://stacks.iop.org/0038-5670/10/i=4/a=R04

[10] M. Pachuilo *et al.*, "Development of a gas-fed plasma source for pulsed high-density plasma/material interaction studies," *IEEE Trans. Plasma Sci.*, vol. 42, no. 10, pp. 3245–3252, Oct. 2014.

[11] A. Mirzabeigy, M. Kalami-Yazdi, and A. Yildirim, "Analytical approximations for a conservative nonlinear singular oscillator in plasma physics," *J. Egyptian Math. Soc.*, vol. 20, no. 3, pp. 163–166, 2012.

[12] L. Gammaitoni, P. Hänggi, P. Jung, and F. Marchesoni, "Stochastic resonance," *Rev. Modern Phys.*, vol. 70, no. 1, p. 223, Jan. 1998.

[13] M. Nurujjaman, A. N. S. Iyengar, and P. Parmananda, "Emergence of the stochastic resonance in glow discharge plasma," *J. Phys., Conf. Ser.*, vol. 208, no. 1, 2010, Art. no. 012084. doi: 10.1088/1742-6596/208/1/012084.

[14] M. M. Badawy, H. A. E.-A. Malhat, S. H. Zainud-Deen, and K. H. Awadalla, "A simple equivalent circuit model for plasma dipole antenna," *IEEE Trans. Plasma Sci.*, vol. 43, no. 12, pp. 4092–4098, Dec. 2015.

[15] G. L. Viviani, "On synthesis and design of multi-stable devices," in *Proc. IEEE Int. Symp. Circuits Syst.*, Espoo, Finland, Jun. 1988, pp.739–742.

[16] Y. Saet and G. Viviani, "The stochastic process of transitions between limit cycles for a special class of self-oscillators under random perturbations," *IEEE Trans. Circuits Syst.*, vol. CAS-34, no. 6, pp. 691–695, Jun. 1987.

[17] Y. A. Saet and G. L. Viviani, "On lienard oscillator models with a pregiven set of limit cycles," *Math. Model.*, vol. 7, nos. 2–3, pp. 377–384, 1986.

[18] L. Perko, *Differential Equations and Dynamical Systems*. New York, NY, USA: Springer-Verlag, 1991.

[19] L. O. Chua and S. M. Kang, "Section-wise piecewise-linear functions: Canonical representation, properties, and applications," *Proc. IEEE*, vol. 65, no. 6, pp. 915–929, Jun. 1977.

[20] (2019). *Weierstrass*. [Online]. Available: https://en.wikipedia.org

[21] R. K. Brayton and J. K. Moser, "A theory of nonlinear networks. I," *Quart. Appl. Math.*, vol. 22, pp. 1–33, 1964.

[22] J. Llibre, M. Ordóñez, and E. Ponce, "On the existence and uniqueness of limit cycles in planar continuous piecewise linear systems without symmetry," *Nonlinear Anal., Real World Appl.*, vol. 14, pp. 2002–2012, Oct. 2013.

[23] J. Llibre, E. Ponce, and C. Valls, "Uniqueness and non-uniqueness of limit cycles for piecewise linear differential systems with three zones and no symmetry," *J. Nonlinear Sci.*, vol. 25, pp. 861–887, Aug. 2015. doi: 10.1007/s00332-015-9244-y.

[24] L. O. Chua and F. Ayrom, "Designing non-linear single OP–AMP circuits: A cook-book approach," *Circuit Theory Appl.*, vol. 13, pp. 235–268, Jul. 1985.

[25] Y. Saet and G. L. Viviani, "Quasilinear and relaxational realms in multiple regime self-oscillators," *Int. J. Non-linear Mech.*, vol. 26, no. 5, pp. 701–709, 1991.

[26] L. E. Dickson, "On quaternions and their generalization and the history of the eight square theorem," *Ann. Math., Second Ser.*, vol. 20, no. 3, Mar. 1919.

[27] S. J. Sangwine, T. A. Ell, and N. Le Bihan, "Fundamental representations and algebraic properties of biquaternions or complexified quaternions," Jan. 2010, *arXiv:1001.0240*. [Online]. Available: https://arxiv.org/abs/1001.0240

[28] E. Noether, "Invariant variation problems," Mar. 2005, *arXiv:physics/0503066*. [Online]. Available: https://arxiv.org/abs/physics/0503066

[29] Y. A. Saet and G. L. Viviani, "An unorthodox paradigm of a relaxational self-oscillator and some classes of nonlinear one-ports," *J. Franklin Inst.*, vol. 322, no. 4, pp. 241–252, 1986.

[30] Y. A. Saet and G. L. Viviani, "A practical algorithm for numerical determination of periodical regimes in nonlinear oscillators," *COMPEL-Int. J. Comput. Math. Elect. Electron. Eng.*, vol. 5, no. 3, pp. 127–136, 1986.

[31] G. L. Viviani and Y. A. Saet, "New type of multi-state detector for adaptive control: An application to network switching," *Int. J. Electron.*, vol. 6, no. 4, pp. 531–533, 1986.

[32] Y. A. Saet and G. L. Viviani, "Multi-stable periodical devices with variations on the theme of van der pol," *J. Franklin Inst.*, vol. 318, pp. 373–382, Dec. 1984.

[33] Y. A. Saet and G. L. Viviani, "On transitions between quasilinear and relaxational regimes in self-oscillators," in *Proc. IEEE Int. Symp. Circuits Syst.*, Jun. 1988, pp. 735–738.

[34] T. R. Blows and L. M. Perko, "Bifurcation of limit cycles from centers and separatrix cycles of planar analytic systems," *SIAM Rev.*, vol. 36, no. 3, pp. 341–376, Sep. 1994.

[35] E. Mishchenko and N. K. Rozov, *Differntial Equations with Small Parameters and Relaxation Oscillations*. New York, NY, USA: Plenum, 1980.

[36] M. W. Hirsch and S. O. Smale, *Differential Equations, Dynamical Systems and Linear Algebra*. New York, NY, USA: Academic, 1974.

[37] A. N. Khondker, M. R. Khan, and A. F. M. Anwar, "Transmission line analogy of resonance tunneling phenomena: The generalized impedance concept," *J. Appl. Phys.*, vol. 63, no. 10, May 1988, Art. no. 5191.

[38] D. Vasileska and G. Klimeck. (2008). *Quantum Mechanics: Harmonic Oscillator*. [Online]. Available: https://nanohub.org/resources/4978

[39] A. Yariv, *Quantum Electronics*, 2nd ed. Hoboken, NJ, USA: Wiley, 1975.

[40] R. Brayton and J. Moser, "Some results on the stability of nonlinear networks containing negative resistance," *IEEE Trans. Circuit Theory*, vol. 11, no. 1, pp. 165–167, Mar. 1964.

[41] J. Hrusak, M. Stork, and D. Mayer, "On brayton-moser network decomposition and state-space energy based generalization of nosé-Hoover dynamics," *WSEAS Trans. Circuits Syst.*, vol. 10, no. 8, pp. 251–266, Aug. 2011.

Gary L. Viviani (SM'86) received the B.S.E.E., M.S.E.E., and Ph.D. degrees from Purdue University, West Lafayette, IN, USA, in 1977, 1978, and 1980, respectively.

He began his work in nonlinear dynamics as a Research Scientist with Central Research at Dupont, Wilmington, DE, USA. He held the GSU Research Professorship (tenured) with Lamar University, Beaumont, TX, USA, where he was involved jointly working with industry to solve complex large-scale control system problems. He was a Principal Engineer with Textron Defense, Wilmington, MA, USA, where he developed autonomous systems with cognitive abilities. He was the Director of Control Systems with Varian Semiconductor, Gloucester, MA, USA, where he was responsible for developing very advanced continuously operating autonomous systems with complete recall and self-recovery capabilities. He also served as Vice President and Chief Scientist for Insitu, Bingen, WA, USA, which is a wholly owned subsidiary of The Boeing Company, Chicago, IL, USA, where he was directly involved with making smaller brains for autonomous robotic airplanes. He is currently a Technical Development Manager with the FAST Labs, BAE Systems, Austin, TX, USA, where he continues his interests in the theory and practice of cognitive devices and other topics.